

# Supramolecular Organization of ssDNA-Templated $\pi$ -Conjugated Oligomers via Hydrogen Bonding

By Mathieu Surin,\* Pim G. A. Janssen, Roberto Lazzaroni, Philippe Leclère, E. W. Meijer, and Albertus P. H. J. Schenning\*

In the frame of supramolecular approaches to organic (nano) electronics, a major challenge is to control the size and the shape of the functional  $\pi$ -conjugated molecular assemblies. Although many bottom-up approaches have been undertaken to direct the self-assembly of  $\pi$ -conjugated (macro)molecules,<sup>[1–8]</sup> so far the majority of the superstructures (e.g., 1D nanowires, fibrils and ribbons, 2D crystals and tapes) lack fine-positioning of the different functional units and monodispersity in the stack length. A few groups reported on the use of a template to control the size of the supramolecular structures.<sup>[1b,3,9]</sup> Especially, oligonucleotides are potentially useful templates or building blocks to construct uniform nano-objects, because of the control in the design of their architecture and the high specificity of the base-recognition process.<sup>[10–13]</sup> Furthermore, the “base-by-base” synthesis of oligonucleotides makes it possible to control both their length and their sequence from a few to more than one hundred bases. Besides base modification<sup>[14]</sup> or the incorporation of  $\pi$ -conjugated oligomers into the DNA backbone by covalent linking,<sup>[15–17]</sup> the use of the H-bonding recognition process in the design of (single-strand) oligonucleotide–chromophore conjugates also appears as an interesting path to prepare monodisperse aggregates.<sup>[18,19]</sup> This approach offers a major advantage: by exploiting the base recognition process, it would be possible to control the sequence of different functional units along the single-strand DNA (ssDNA). This templating approach based on H-bonding has been exploited by Iwaura et al. to organize thymine-capped (bola)amphiphiles, for example, a water-soluble  $\pi$ -conjugated oligo(*p*-phenylene vinylene) derivative that binds between two strands of oligoadenine.<sup>[18]</sup>

Complementary to a templated approach using H-bonded guanosine scaffolds,<sup>[20]</sup> we recently reported on the design of a water-soluble naphthalene and a oligo(*p*-phenylene vinylene) guest derivatives end-capped with one diaminotriazine (DT) H-bonding unit, which binds to a single-strand oligothymine template (oligothymine 40-mer, dT<sub>40</sub>) in aqueous solution. The

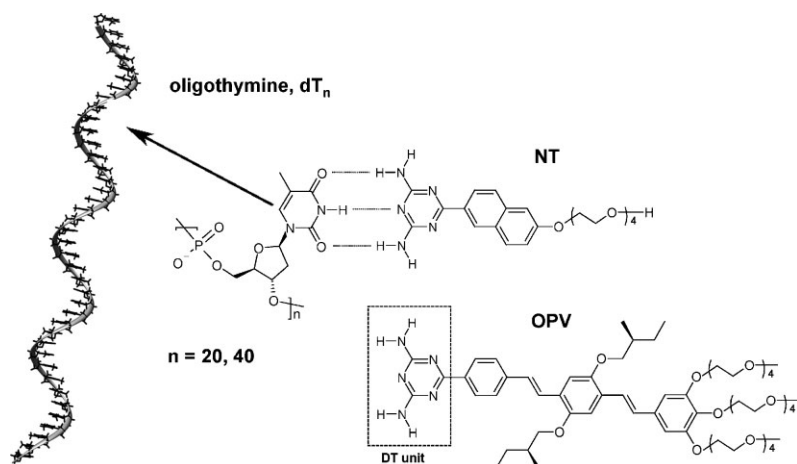
self-assembly leads to right-handed helical hybrid structures, as indicated by circular-dichroism (CD) spectroscopy.<sup>[19]</sup> Although the spectroscopic data indicate the presence of fully-bound complexes (one guest for each thymine of the ssDNA), detailed information on the influence of the molecular structure of the guest on the structural order and intermolecular interactions in those systems is lacking. In this communication, we report on the supramolecular organization in these hybrid assemblies composed of a oligothymine template (dT<sub>n</sub>) with a naphthalene or an oligo(*p*-phenylene vinylene) derivative equipped with a diaminotriazine unit (NT or OPV, respectively, see Scheme 1). In this joint theoretical and experimental approach, atomistic modeling based on molecular dynamics (MD) is carried out to propose structural models that can be related to CD spectroscopy and tapping-mode atomic force microscopy (TM-AFM) measurements. A better understanding of the nature and amplitude of the intermolecular interactions is essential for exploiting these functional supramolecular structures.

To get insight into the base recognition process towards a non-natural diaminotriazine (DT) unit, molecular mechanics (MM) calculations on H-bonded dimers (thymine–DT, adenine–thymine, adenine–DT, DT–DT) have been used to estimate the relative binding energies. The binding energy and the H-bonding contribution (defined as the total and H-bond energies of the dimer minus those of individual molecules) have been estimated using different force fields, including the Chemistry at Harvard macromolecular mechanics (CHARMM) force field for nucleic acids,<sup>[21]</sup> which is then used for simulating the studied structures (see Supporting Information). Although these energy values have no absolute meaning, the comparison for a given force field provides a reliable estimate of the strength of the interactions: among the four possible dimers, the triply hydrogen-bonded thymine–diaminotriazine (T–DT) is the most stable structure, stabilized by at least  $-3.5 \text{ kcal mol}^{-1}$  ( $-14.6 \text{ kJ mol}^{-1}$ ), compared to the other possible H-bonded dimers, where only two H-bonds are possible, including the adenine–thymine (A–T) dimer. Concerning the interaction between chromophores in a cofacial conformation, naphthalene molecules have a tendency to  $\pi$ -stack in a parallel displaced arrangement at a distance of around 0.37 nm. The binding energy between two naphthalene molecules ( $-4 \text{ kcal mol}^{-1}$ ) is clearly smaller than the binding-energy values for the T–DT H-bonding dimer ( $-13.5 \text{ kcal mol}^{-1}$ ). In contrast, the binding energy between two stacked oligo(*p*-phenylene vinylene) with chiral substituents ( $-29 \text{ kcal mol}^{-1}$ ) is much larger than the interaction within the T–DT dimer. In this case, the adjacent OPVs are stacked at a distance of 0.37 nm in a “crossed” conformation, with

[\*] Dr. M. Surin, Prof. R. Lazzaroni, Dr. P. Leclère  
Laboratory for Chemistry of Novel Materials  
Université de Mons-Hainaut  
20 Place du Parc, 7000 Mons (Belgium)  
E-mail: Mathieu@averell.umh.ac.be

Dr. A. P. H. J. Schenning, P. G. A. Janssen, Prof. E. W. Meijer  
Laboratory for Macromolecular and Organic Chemistry  
Technische Universiteit Eindhoven  
P.O. Box 513, 5600 MB Eindhoven (The Netherlands)  
E-mail: A.P.H.J.Schenning@tue.nl

DOI: 10.1002/adma.200801701



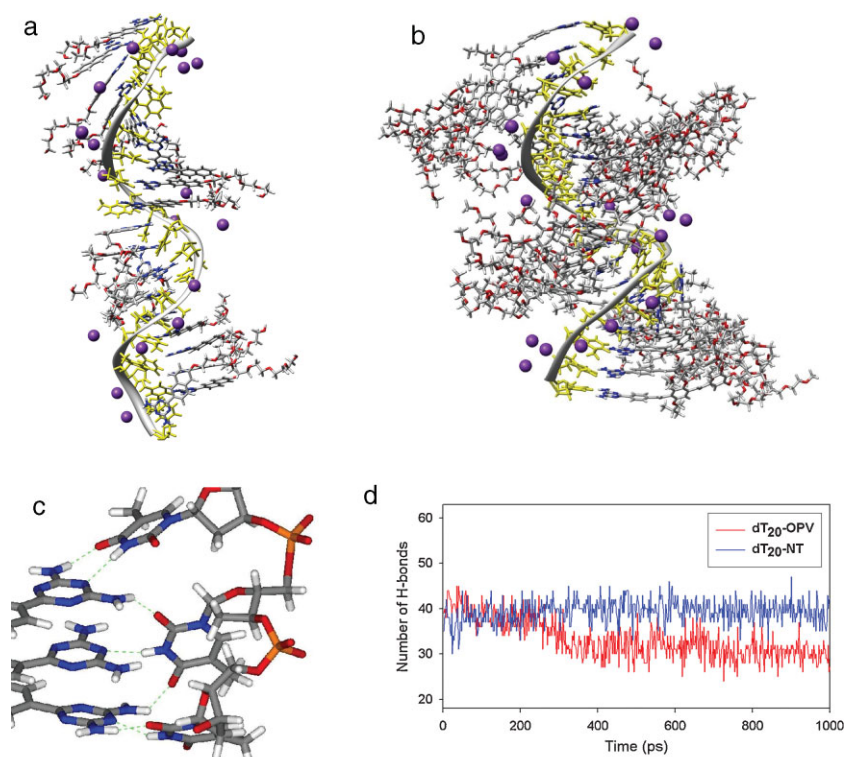
**Scheme 1.** Chemical structures of the compounds studied.

a rotation angle of around  $40^\circ$  between the OPVs axes (see Supporting Information) due to the chiral (*S,S'*) 2-methylbutoxy substituents on the phenylene ring at the center of the OPV segment.<sup>[22]</sup>

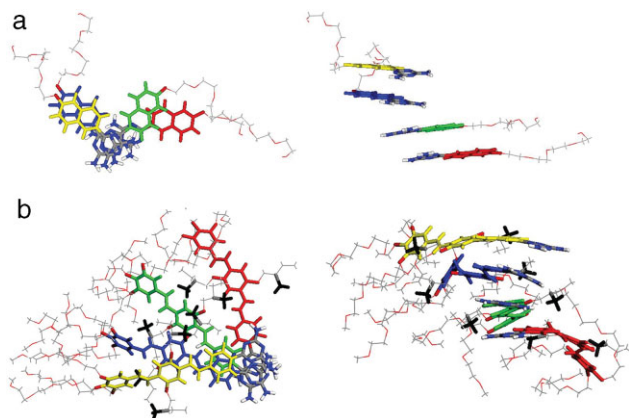
MD simulations on the nanosecond timescale for the fully-bound complex between NT or OPV and single-strand  $dT_{20}$  or  $dT_{40}$  templates were carried out starting from a B-helix in the generalized Born implicit water-solvent model, and taking into account sodium counter-ions along the ssDNA backbone.<sup>[23]</sup>

Figure 1 shows snapshots for the  $dT_{20}$ -NT and  $dT_{20}$ -OPV structures taken at the end of the MD run. In both cases, right-handed helices are stable structures, in agreement with CD spectra showing a positive Cotton effect on the low energy side (Fig. 3a). For  $dT_{20}$ -NT, the stable conformations display one helical turn every 10 thymine units, corresponding to a pitch of about 3.5 nm, similar to the B-type helix of a double-strand DNA, suggesting that the template dominates the conformation. Concerning the chromophore stacking, the naphthalene units are almost perpendicular to the strand axis, but their planes are not strictly parallel to each other, because of the flipping of the bases during the MD run (see below). On average, the rotation per base pair is  $36^\circ$ , and in most cases there is almost no overlap between the benzene rings of neighboring NT units (see red, green, and blue naphthalenes in Fig. 2a), except for a few units over the entire complex (see blue and yellow naphthalenes in Fig. 2a). The inter-naphthalene distance in those stacks fluctuates at around 0.5 nm, and the ethylene oxide end-groups are rather extended, having little interaction with each other. For  $dT_{20}$ -OPV, MD shows stable structures with one helical turn every 14–15 thymines, corresponding to a 4.6 nm pitch (see Fig. 1b). The OPV backbones are relatively parallel

(see Fig. 2b), with an average distance between benzene rings of neighboring OPV ranging between 0.4 and 0.5 nm. The ethylene oxide end-groups are coiled, in a few cases they are folded in between neighboring OPV segments. The alkyl side-groups on the central phenylene rings of OPV segments show no preferential orientation; the methyl groups (in black sticks in Fig. 2b) are randomly oriented, which suggests that the presence of chiral centers (here, *S,S'*) does not influence the supramolecular organization in those stacks. The difference in length of the complex (7.0 nm for  $dT_{20}$ -NT and 6.7 nm for  $dT_{20}$ -OPV) and the helical pitch between the structures with NT and OPV can be rationalized when comparing the stacking interactions between guests. For NT, the weak interaction between conjugated units does not alter the 'natural' structure of the DNA backbone (average rotation per "base pair" of  $36^\circ$ ), while stronger interactions between guests, and larger steric effects (larger content of flexible, saturated groups), impose a significantly distorted DNA structure in the case of OPV (average rotation per "base pair" around  $25^\circ$ ). For comparison, the estimated average binding energy between adjacent naphthalenes in  $dT_{20}$ -NT is on the order of  $-1.1 \text{ kcal mol}^{-1}$ , while for adjacent oligo(*p*-phenylene vinylene)



**Figure 1.** a,b) Snapshots at the end of MD for a)  $dT_{20}$ -NT and b)  $dT_{20}$ -OPV (stick view, single strand in yellow with ribbon,  $\text{Na}^+$  ions as purple balls). c) Close-up view of three thymines binding three DT units (H-bonds in dashed light blue). d) Evolution of the number of H-bonds during the MD run for the  $dT_{20}$ -NT and  $dT_{20}$ -OPV structures.



**Figure 2.** Line and stick model of clusters of four guest chromophores, extracted from the structures shown in Figure 1. The adjacent a) NT and b) OPV units are shown in different colors, with axis parallel (left) and perpendicular (right) to the view. The methyl groups of chiral carbon atoms are in black.

segments in dT<sub>20</sub>-OPV this value amounts to around  $-8.6 \text{ kcal mol}^{-1}$ .

The higher stacking interaction energy in the hybrid complex between OPV units compared to NT units is also observed in a temperature-dependent self-assembly experiment monitored with CD, see Figure 3. When OPV or NT are mixed with dT<sub>20</sub> or dT<sub>40</sub>, a positive Cotton effect in the chromophore absorption region is observed, indicative of binding to the ssDNA template (Fig. 3 and Supporting Information). Upon slowly cooling the solutions containing OPV or NT with dT<sub>40</sub> and monitoring the positive CD maximum, where only the chromophores absorb, the OPV molecules bind to the dT<sub>40</sub> at a higher temperature, suggesting a more stable hybrid structure, caused by an increased stacking interaction between guest molecules. Moreover, the steeper slope change in the temperature-dependent CD spectra for the dT<sub>40</sub>-OPV compared to dT<sub>40</sub>-NT (Fig. 3b) suggests a higher enthalpy of the self-assembly, induced by a stronger stacking interaction between adjacent guest molecules.<sup>[24]</sup>

From the MD simulations, we clearly observe in both structures multiple H-bonds between each diaminotriazine unit and adjacent thymine units, due to base 'flipping' (usually referred to as 'shear', 'buckle,' and 'propeller twist' in helical coordinates for double-stranded DNA), like, for instance, Figure 1c shows that a single thymine can be H-bonded to three diaminotriazines. Figure 1d shows the evolution of the number of intermolecular H-bonds in the complexes of dT<sub>20</sub> with NT or OPV during the MD run (simulation carried out at 298 K<sup>[25]</sup>). In the initial conformation for the MD simulation, 60 H-bonds are present (three per base pair). Base flipping during the early MD heating and relaxation periods reduces the number of intermolecular H-bonds to around 40 in both structures (this stage is defined as 0 ps in Fig. 1d). For the dT<sub>20</sub>-NT, the structure evolves, maintaining that average value of 40 H-bonds for the entire MD run. For dT<sub>20</sub>-OPV, after a MD time of 0.3 ns, the structure stabilizes with about 30 H-bonds, that is, half of the maximum value. Again, this difference originates from interguest interactions in the stacks. It is remarkable that in the structure with OPV, the stacking interaction prevails on the H-bonding interaction

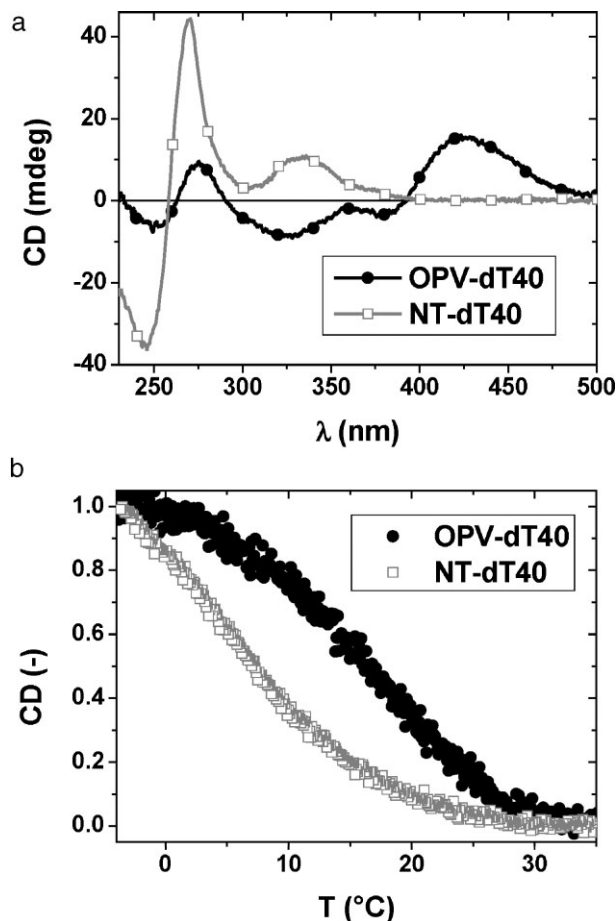


**Figure 3.** a) CD spectra at 0 °C and b) normalized temperature-dependent CD signal of dT<sub>40</sub>-OPV or dT<sub>40</sub>-NT mixtures in water containing 2% dimethyl sulfoxide (DMSO), measured by cooling with 1 °C min<sup>-1</sup> at 420 nm or 323 nm respectively. [OPV] = 0.25 mM, [NT] = 0.25 mM, [dT<sub>40</sub>] = 6.25 μM.

(i.e., some H-bonds are broken in favor of better  $\pi$ -stacking), while the opposite occurs in the structure with NT. In both cases, the static view of one guest binding perpendicular to the single strand axis with three H-bonds per monomer is misleading: the flipping of the bases leads to several types of H-bonding patterns between neighboring DT and T bases, which therefore induces conformational disorder in the guests stacks. The higher interactions between the guest molecules are at the cost of the influence of the template on the structural order and the hydrogen-bond interaction between the guest and the template. The effect of the length of the template on the supramolecular ordering was studied for NT bound to dT<sub>20</sub> and dT<sub>40</sub>. Whatever the length, no change in the helix pitch is observed in the MD simulations. However, more structural disorder is observed for complexes with a smaller template: the distance between conjugated units shows large variations for dT<sub>20</sub> compared to dT<sub>40</sub> templates. The higher structural order for the larger template results in a higher degree of hydrogen bonding, in average: 2 versus 2.3 H-bonds per thymine for dT<sub>20</sub> and dT<sub>40</sub>, respectively. This effect is under study, and detailed simulations

of the CD spectra<sup>[26]</sup> based on the molecular models are underway.

In order to characterize the morphology of individual complexes, the adsorption of these supramolecules on surfaces is studied using TM-AFM in a liquid solution, revealing directly the structure within the solution mixture at concentrations where 1:1 binding takes place (in the 0.1–1.5 mM range<sup>[19]</sup>), without forming a thick layer on the substrate surface. The substrate is a Mg<sup>2+</sup>-modified mica surface, allowing the strong adsorption of negatively-charged DNA molecules.<sup>[27]</sup> Aqueous mixtures of NT with a dT<sub>40</sub> template deposited on this surface show globular structures with a thickness of around 2.7 nm (Fig. 4a), but the attainable resolution available with this setup does not allow the discrimination of the long and short axes of the complexes. In order to verify whether the observed objects are the dT<sub>40</sub>-NT complexes, we use a ssDNA-polythymine template, dT<sub>p</sub>. When mixing this template with NT (dT<sub>p</sub>-NT complex), we observe coiled wire-like objects (Fig. 4b) that have the same thickness as with dT<sub>40</sub>, that is, (2.8 ± 0.5) nm. However, the length of the dT<sub>p</sub>-NT structures ranges from around 100 nm to 700 nm, corresponding to a few hundreds to up two thousand bases. Note that for the pure dT<sub>p</sub>, the measured thickness of the observed single strands is around (0.9 ± 0.2) nm. Surprisingly, for the mixture of dT<sub>40</sub> with OPV, micrometer-long wires form on the modified mica surface. Figure 4c shows one such micrometer-long curved wire, with a thickness of (4.5 ± 0.5) nm. The fact that those structures are much longer than the dT<sub>40</sub> template (around 14 nm) implies that long-range interactions occur between dT<sub>40</sub>-OPV complexes, probably as a result of the stronger interactions between the OPV units (compared to the NT units), which makes the complexes aggregate along the strand axis. Notably, these wires do not arise from assembly of pure conjugated oligomers, for which deposits display untextured aggregates or platelet-like assemblies. The thickness of the observed structures in aqueous media is in good agreement with the width of structures, as expected from molecular modeling: the average diameters in the MD models are around 3.5 nm for the complex with NT and 5.0 nm for that with OPV, and the observed thicknesses are (2.8 ± 0.5) and (4.5 ± 0.5) nm, respectively (see cross-sections in Fig. 4). The slight difference between the molecular models and the AFM measurements most likely arises from the strong adsorption of the complex on the modified mica surface (the DNA backbone and the ethylene oxide groups both have strong affinity with ions present at the surface), and/or from slight compression of the complex with the AFM tip. The observed widths of the wires (around 30 nm for the complex with NT and around 45 nm for that with OPV) also corresponds to the expected width, considering the convolution with a tip radius of curvature of 15–20 nm.<sup>[27]</sup> This is clear evidence of the adsorption of the fully-bound H-bonded complexes to the surface. The fact that we do not observe the helical conformation is due to the resolution limit in these experimental conditions.

In conclusion, molecular modeling simulations of the organization of conjugated oligomers, ssDNA H-bonded complexes, provide detailed structural information, which is a key issue for the understanding of dominant interactions in such structures. An important observation is that, for larger interactions between the guests in the complex, the H-bond interaction between the guests and the template diminishes, and the stacking

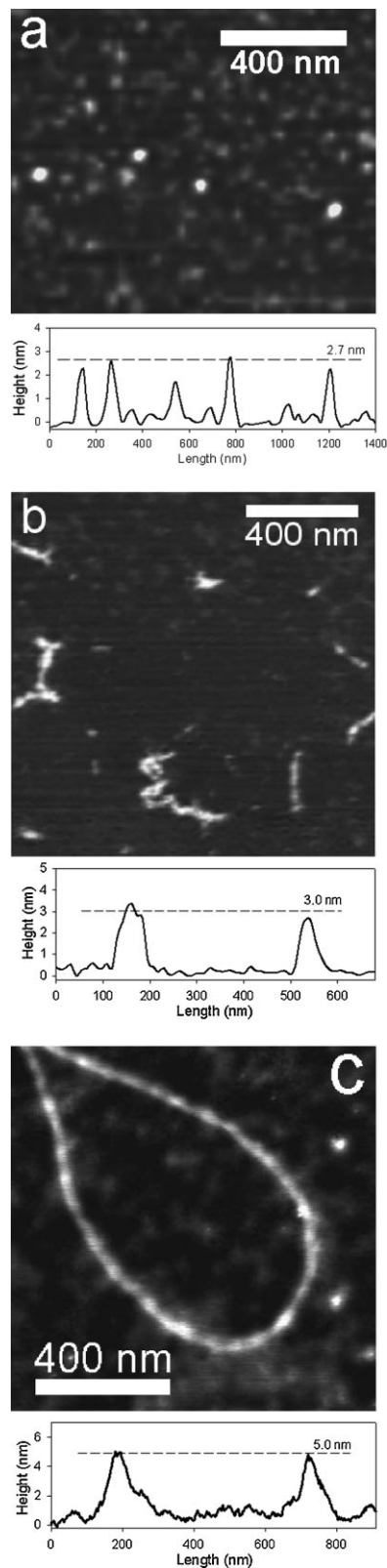


**Figure 4.** Liquid-cell TM-AFM height images of aqueous mixtures deposited on Mg<sup>2+</sup>-mica surfaces of a) [dT<sub>40</sub>] = 10 μM and [NT] = 0.4 mM, b) [T]<sub>dTn</sub> = 0.25 mM and [NT] = 0.5 mM, and c) [dT<sub>40</sub>] = 0.125 mM and [OPV] = 0.25 mM. The plots at the bottom of images are cross-sections across the wires.

of guests will have stronger influence on the structure of the template. The AFM studies have revealed that the assembly on surface and the persistence length of these complexes is also determined by the interaction between the guest molecules. For large interactions between conjugated molecules in the stacks, the complex can further aggregate along the strand axis. These insights are important for the future design of templated multichromophoric assemblies, and the understanding of their spectroscopic properties, for instance, electron-donor and -acceptor conjugated units (e.g., OPV and perylene derivatives, respectively) carrying different H-bonding moieties can be aligned and fine-positioned with a sequence determined by the sequence of oligonucleotide complementary bases, which would be of great interest to better understand energy- and charge-transfer processes between different chromophores.

## Experimental

The experimental section can be found in the Supporting Information.

## Acknowledgements

The work in Mons is supported by the Belgian Federal Science Policy Office (PAI 6/27) and the Belgian National Fund for Scientific Research (FNRS/FRFC). M. S. and P. L. are Chargé de Recherches and Chercheur Qualifié of the F.R.S.-FNRS (Belgium), respectively. The work in Eindhoven is supported by a EURYI grant of the European Science Foundation and by the Chemical Council of the Netherlands Organization of Scientific Research (NWO). Supporting Information is available online from Wiley InterScience or from the authors.

Received: June 19, 2008

Revised: October 2, 2009

Published online: December 12, 2008

- [1] a) B. W. Messmore, J. F. Hulvat, E. D. Sone, S. I. Stupp, *J. Am. Chem. Soc.* **2004**, *126*, 14452. b) S. R. Bull, L. C. Palmer, N. J. Fry, M. A. Greenfield, B. W. Messmore, T. J. Meade, S. I. Stupp, *J. Am. Chem. Soc.* **2008**, *130*, 2742.
- [2] P. Leclère, M. Surin, P. Brocorens, M. Cavallini, F. Biscarini, R. Lazzaroni, *Mater. Sci. Eng. R* **2006**, *55*, 1.
- [3] O. Ikkala, G. ten Brinke, *Chem. Commun.* **2004**, 2131.
- [4] F. J. M. Hoeben, P. Jonkheijm, E. W. Meijer, A. P. H. J. Schenning, *Chem. Rev.* **2005**, *105*, 1491.
- [5] J. A. A. W. Elemans, R. van Hameren, R. J. M. Nolte, A. E. Rowan, *Adv. Mater.* **2006**, *18*, 1251.
- [6] L. Sardone, V. Palermo, E. Devaux, D. Credgington, M. De Loos, G. Marletta, F. Cacialli, J. van Esch, P. Samori, *Adv. Mater.* **2006**, *18*, 1276.
- [7] E. Gomar-Nadal, J. Puigmarti-Luis, D. B. Amabilino, *Chem. Soc. Rev.* **2008**, *37*, 490.
- [8] a) E. Jahnke, N. Severin, P. Kreutzkamp, J. P. Rabe, H. Frauenrath, *Adv. Mater.* **2008**, *20*, 409. b) H. Frauenrath, E. Jahnke, *Chem. Eur. J.* **2008**, *14*, 2942.
- [9] T. Sugimoto, T. Suzuki, S. Shinkai, S. K. Sada, *J. Am. Chem. Soc.* **2007**, *129*, 270.
- [10] T. H. LaBean, H. Li, *Nanotoday* **2007**, *2*, 26.
- [11] P. W. K. Rothmund, *Nature* **2006**, *440*, 297.
- [12] B. Samori, G. Zuccheri, *Angew. Chem. Int. Ed.* **2005**, *44*, 1166.
- [13] N. C. Seeman, *Nature* **2003**, *421*, 427.
- [14] K. Tanaka, A. Tengeiji, T. Kato, N. Toyama, M. Shionoya, *Science* **2003**, *299*, 1212.
- [15] a) F. D. Lewis, L. G. Zhang, X. Y. Liu, X. B. Zuo, D. M. Tiede, H. Long, G. C. Schatz, *J. Am. Chem. Soc.* **2005**, *127*, 14445. b) F. D. Lewis, L. G. Zhang, X. B. Zuo, *J. Am. Chem. Soc.* **2005**, *127*, 10002.
- [16] M. A. Abdalla, J. Bayer, J. O. Radler, K. Müllen, *Angew. Chem. Int. Ed.* **2004**, *43*, 3967.
- [17] W. Wang, W. Wan, H. H. Zhou, S. Q. Niu, A. D. Q. Li, *J. Am. Chem. Soc.* **2003**, *125*, 5248.
- [18] a) R. Iwaura, K. Yoshida, M. Masuda, M. Ohnishi-Kameyama, M. Yoshida, T. Shimizu, *Angew. Chem. Int. Ed.* **2003**, *42*, 1009. b) R. Iwaura, F. J. M. Hoeben, M. Masuda, A. P. H. J. Schenning, E. W. Meijer, T. Shimizu, *J. Am. Chem. Soc.* **2006**, *128*, 13298.
- [19] P. G. A. Janssen, J. Vandenbergh, J. L. J. van Dongen, E. W. Meijer, A. P. H. J. Schenning, *J. Am. Chem. Soc.* **2007**, *129*, 6078.
- [20] G. P. Spada, S. Lena, S. Masiero, S. Pieraccini, M. Surin, P. Samori, *Adv. Mater.* **2008**, *20*, 2433.
- [21] a) A. D. Mackerell, J. Wiorkiewicz-Kuczera, M. Karplus, *J. Am. Chem. Soc.* **1995**, *117*(1), 1946. b) F. A. Momany, R. Rone, *J. Comput. Chem.* **1992**, *13*, 888. c) A. D. Mackerell, N. Banavali, N. Foloppe, *Biopolymers* **2000**, *56*, 257.
- [22] For a stack of H-bonded dimers of OPV4 (with a quadruple H-bonding unit), the rotation angle between adjacent units is around 6–12°, as estimated using the Dreiding force field, see: D. Beljonne, E. Hennebicq, C. Daniel, L. M. Herz, C. Silva, G. D. Scholes, F. J. M. Hoeben, P. Jonkheijm, A. P. H. J. Schenning, S. C. J. Meskers, R. T. Phillips, R. H. Friend, E. W. Meijer, *J. Phys. Chem. B* **2005**, *109*, 10594. The difference with the value of 40° found here comes from the fact we do not take into account H-bonding dimers, but only stacks of OPV units with the central chiral groups.
- [23] MD simulations were carried out starting from the B-helix structure extracted from a A<sub>n</sub>-T<sub>n</sub> double-strand DNA. Simulations on single-strand dT<sub>40</sub> with Na<sup>+</sup> counter-ions show results in accordance with a) S. Sen, L. Nilsson, *J. Am. Chem. Soc.* **2001**, *123*, 7414 and b) J. M. Martinez, S. K. C. Elmroth, L. Kloo, *J. Am. Chem. Soc.* **2001**, *123*, 12279.
- [24] The dT<sub>40</sub>-OPV disassembly is also more difficult than the dT<sub>40</sub>-NT disassembly: the hysteresis of the dT<sub>40</sub>-OPV disassembly is larger, which also supports an increased stability.
- [25] Note that the average number of H-bonds in the studied complexes varies with the temperature used in the MD simulation. Here we only show the results for MD performed at 298 K.
- [26] F. C. Spano, S. C. J. Meskers, E. Hennebicq, D. Beljonne, *J. Am. Chem. Soc.* **2007**, *129*, 7044.
- [27] C. Bustamante, J. Vesenska, C. L. Tang, W. Rees, M. Guthold, R. Keller, *Biochemistry* **1992**, *31*, 22.